

Revised optical classification of “LINERs”

H. V. Abrahamyan, A. M. Mickaelian, G. A. Mikayelyan, G. M. Paronyan

NAS RA V. Ambartsumian Byurakan Astrophysical Observatory (BAO), Armenia

E-mail: abrahamyanhayk@gmail.com

Abstract

This work is dedicated to reclassification of LINERs. For our investigation we use the catalogue Véron-Cetty & Véron 13th edition. In this catalogue 926 LINERs are included. Cross-correlation of these sources with SDSS DR14 gives 176 objects which have spectra in SDSS. Having medium-resolution spectra from SDSS we have done reclassification of these sources. As a result, 54% of these sources have changed their classification.

Keyword: *LINER, Seyfert, HII, AGN, classification.*

1. Introduction

The first catalogue of quasars was published in 1971 by De Veny et al. and it contained 202 objects. Since 1984 until 2010 this work was continued by Véron-Cetty & P. Véron who published 13 editions. In this period many works have been done leading to the discovery of many many quasars. The release of both the 2dF catalogue (Croom et al. 2001, 2004) and the first four data releases (Abazajian et al. 2003, 2004, 2005; Adelman-McCarthy et al. 2006) of the Sloan Digital SkySurvey (Fan et al. 1999) has increased the number of known quasars. In Véron-Cetty & P. Véron (herewith VCV-13, 2010) catalogue quasars have almost doubled from SDSS DR5, DR6 and DR7 releases (Adelman-McCarthy et al. 2007, 2008; Abazajian et al. 2009). VCV-13 catalogue includes 168,940 quasars and other active galactic nuclei (Table 1).

Low-ionization nuclear emission line region (**LINER**) is a type of galactic nucleus which is defined by its spectral line emission. The spectra typically include line emission from weakly ionized or neutral atoms. Conversely, the spectral line emission comes from strongly ionized atoms. Galaxies that contain LINERs are often referred to as LINER galaxies. LINER galaxies are very common; approximately one-third of all nearby galaxies (at approximately 25-45 Mpc distances) may be classified as LINER galaxies. Approximately 75% of LINER galaxies are either elliptical

galaxies, lenticular galaxies, or spiral galaxies (S0/a-Sab). LINERs are found less frequently in Sb-Scd galaxies, and they are very rare in nearby irregular galaxies. LINERs also may be commonly found in luminous infrared galaxies (LIRGs), a class of galaxies defined by their infrared luminosities that are frequently formed when two galaxies collide with each other. Approximately one-quarter of LIRGs may contain LINERs.

Table 1. Distribution of the activity types in VCV-13.

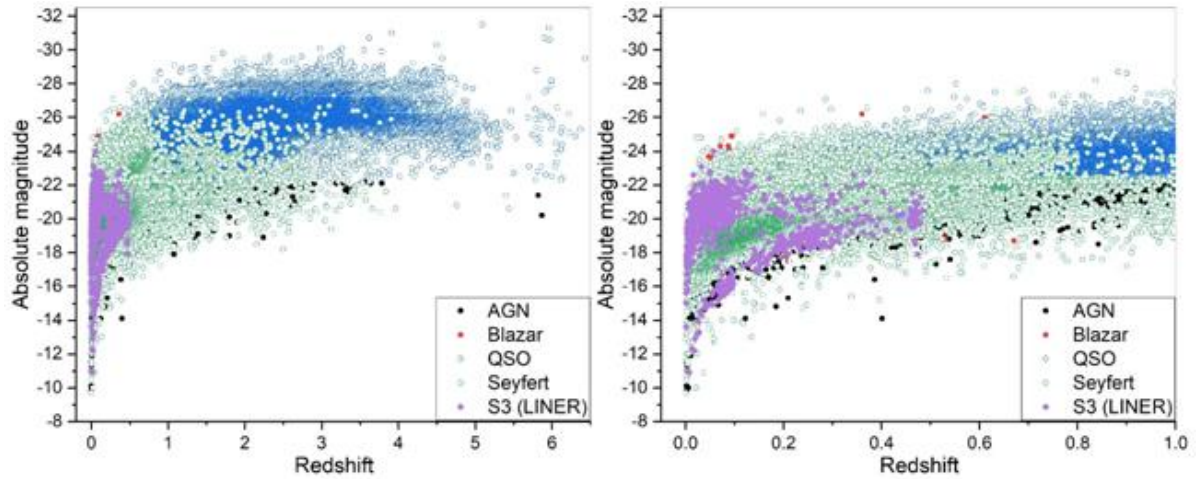
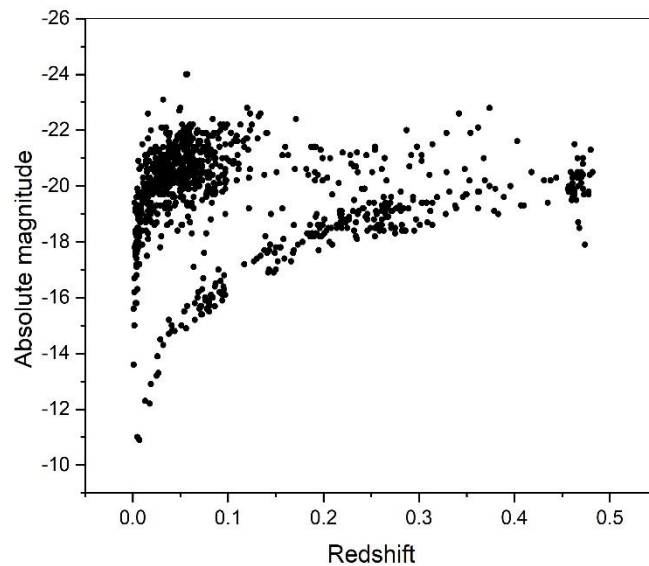
Classification	Numbers		Classification	Numbers
Blazar	1,307		HII	167
S	417		HP	148
S?	342		Q2	17
S1	16,178		Q?	11
S1.0	198		L	1
S1.2	197		AGN	9,888
S1.5	462		QSO	129,750
S1.8	159			
S1.9	195			
S1h	45			
S1i	13			
S1n	2,333			
S2	6,186			
S3 (LINER)	926			
Total				168,940

2. Observing data

Our work is dedicated to revised optical classification of LINERs using SDSS spectra. These LINERs are taken from VCV-13 catalogue. SDSS gives medium resolution spectra for our sources and gives opportunity to do better classification than before.

For our investigation we have 926 LINERs from VCV-13 (Table 1). In figure 1 we can see the dependence of absolute magnitudes on redshift.

From figure 1 and 2 it is possible to conclude that LINERs are divided into 2 parts. We can suppose LINERs have 2 subtypes (higher and lower luminosity LINERs?). However, for understanding if LINERs have 2 subtypes, we must have more information for these objects. In this work we will not discuss these subtypes and will focus on the classification of LINERs.

**Figure 1.** Absolute magnitude vs. redshift**Figure 2.** Absolute magnitude vs. redshift for LINERs

In table 2 we give information of apparent and absolute magnitudes and redshifts for LINERs from VCV - 13 catalogue.

Table 2. LINERs' magnitude and redshift.

Redshift		V magnitude		Absolute magnitude		Numbers
Range	Average	Range	Average	Range	Average	926
0.001÷0.482	0.116	9.25÷22.8	17.07	-10.9÷-24	-19.77	

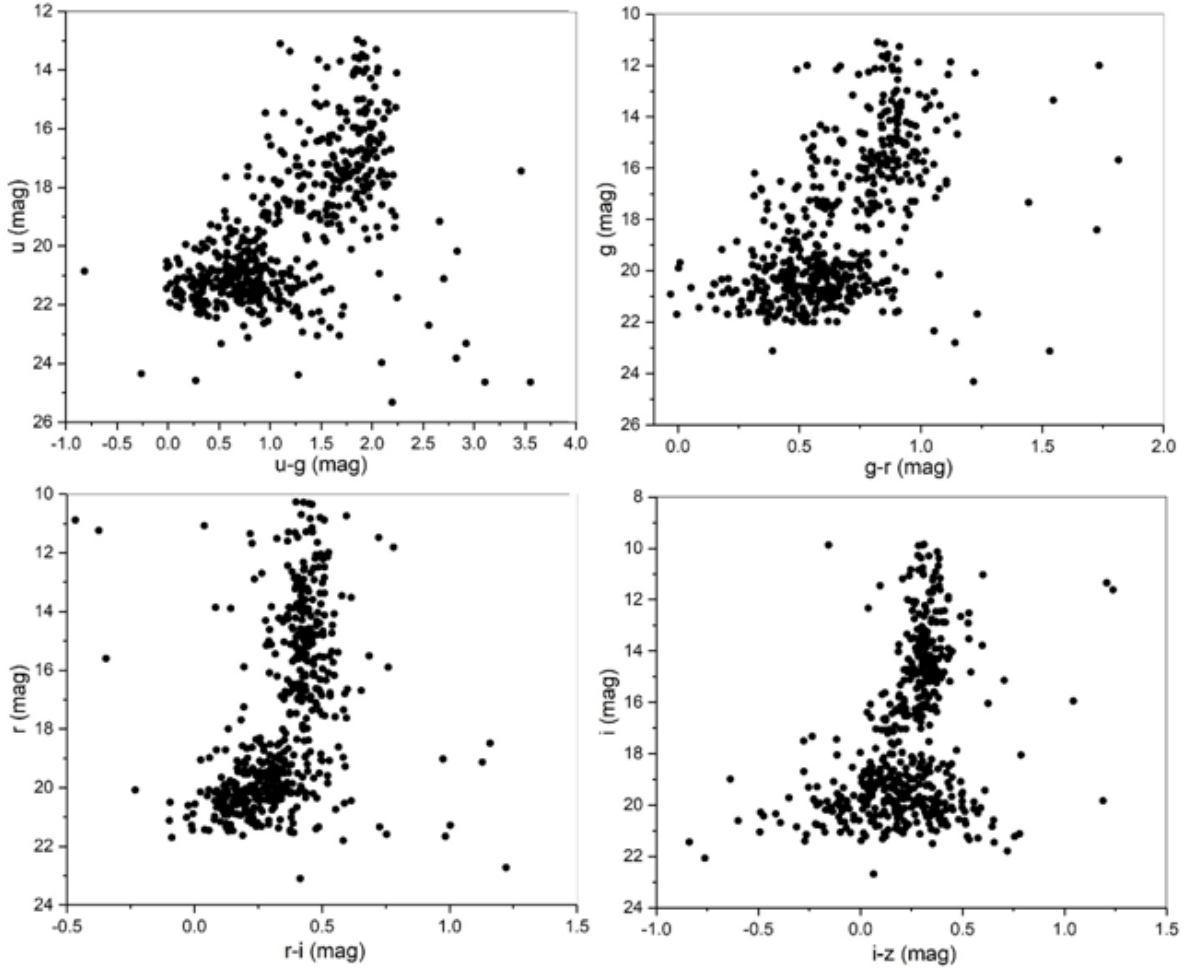


Figure 3. Color-magnitude diagrams for LINERs.

For our investigation we have carried out cross-correlation with SDSS DR14 and as a result we have 176 LINERs, which have medium resolution spectra. These spectra allow reclassification for these objects. The wavelength range for all spectra is 3800-9200Å. As SDSS observations have used the same size of the fiber, most of the resolved galaxies appeared to have absorption components and only very few show pure nuclear spectra. Most typical absorption lines are Mg II 5175Å, Na I 5890Å and Balmer lines among which most important are H β absorption components superposed on the emission components coming from nuclei. Due to redshifts in the SDSS spectral range usually appear the following emission lines: [OII] 3727Å, [Nelli] 3869Å, H ζ /Hel 3889Å, [Nelli] 3968Å, H ϵ , [SII] 4069/76Å, H δ , H γ , [OIII] 4363Å, Hel 4471Å, Hell 4686Å, H β , [OIII] 4959Å, [OIII] 5007Å, NI 5198/5200Å, [NII] 5755Å, Hel 5876Å, [FeVII] 6087Å, [OI] 6300Å, [OI] 6364Å, [NII] 6548Å, H α , [NII] 6583Å, Hel 6678Å, [SII] 6716Å, [SII] 6731Å, Hel 7065Å, [Ar III] 7136Å, [ArIV] 7237Å, [OII] 7319Å, [OII] 7329Å. Very often SDSS measurements from their spectra are based on very low quality lines at the level of noise. These automatic measurements give some artificial numbers that indicate non-real data. So one needs to carefully check the spectra

along all wavelengths and decide which measurements should be used for further studies. Especially important are those, which are being used in the diagnostic diagrams ($H\beta$, [OIII] 5007Å, [OI] 6300Å, $H\alpha$, [NII] 6583Å) (L. C. Ho et al. 1997).

Having information of magnitude from SDSS DR14 catalogue we build color-magnitude diagrams for LINERs (figure 3). In figure 3 we can see 2 concentrations of LINERs, which can be described as follows: 1) LINERs have 2 subtypes and 2) wrong classification of these sources was done. Having 176 medium resolution spectra we show that mostly wrong classification of these sources was done using older low-resolution spectra.

3. Classification method

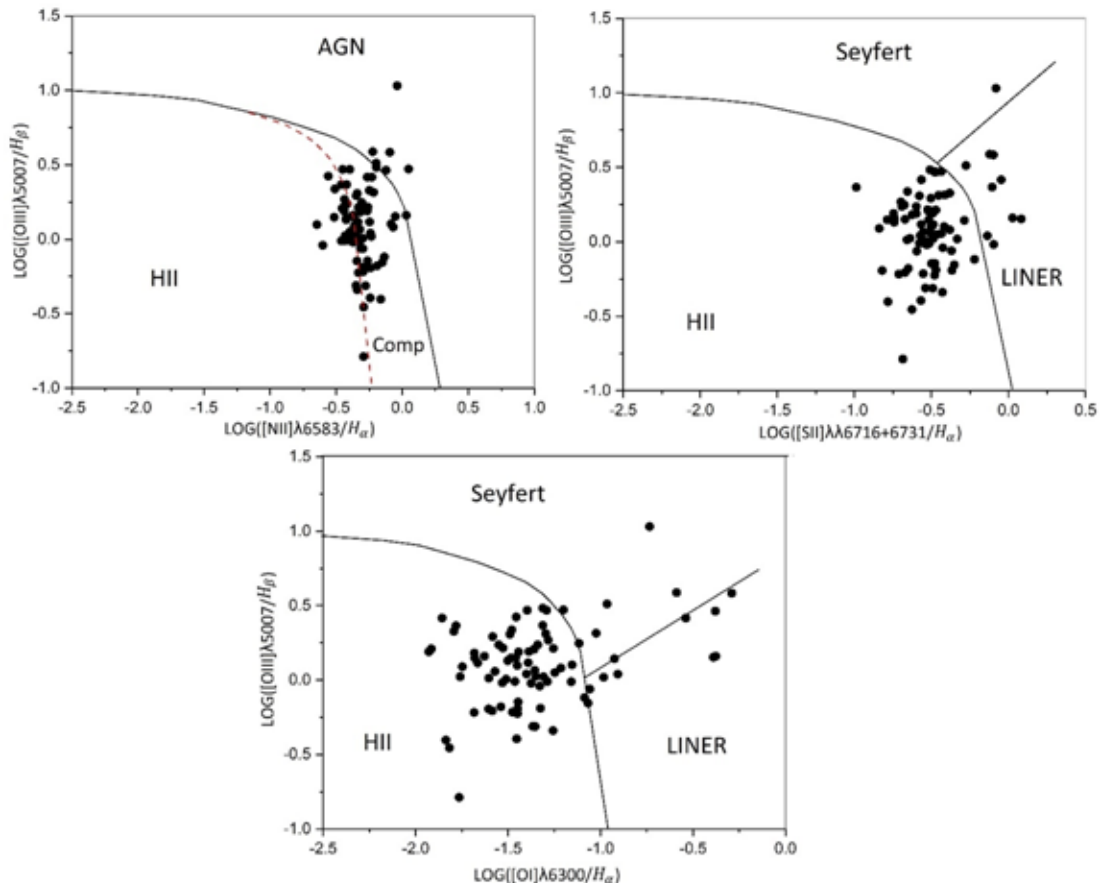


Figure 4. Diagnostic diagrams for LINERs.

We have used several methods for classification of our spectra (Mickaelian et al. 2018);

- By eye (taking into account all features and effects)
- By diagnostic diagram using $[\text{OIII}]/H_{\beta}$ and $[\text{NII}]/H_{\alpha}$ ratios (figure 4),
- By diagnostic diagram using $[\text{OIII}]/H_{\beta}$ and $[\text{SII}]/H_{\alpha}$ ratios (figure 4),

- By diagnostic diagram using $[\text{OIII}]/H_{\beta}$ and $[\text{OI}]/H_{\alpha}$ ratios (figure 4),
- Using together 1st, 2nd and 3rd diagnostic diagrams (Reines, Amy E. et al. 2013).

Classification by eye has been done to compare with the classification by diagnostic diagrams and because not all objects appeared on them. Roughly, we distinguish Seyferts from LINERs by the criteria: $[\text{OIII}]/H_{\beta} > 4$, and AGN from HII by $[\text{SII}]/H_{\alpha} > 2/3$, $[\text{OI}]/H_{\alpha} > 0.1$ criteria.

So, mostly our sources changed their classification (table 3). On Figure 5 we give examples of spectra for some activity type.

4. Results of Study of the Spectra and Classification

We started the studying of spectra with identifications of spectral lines. We have used only lines having intensities 3σ over the noise level. H_{β} also appears in absorption on most of these spectra. We studied the influence of H_{β} absorption component on the emission one, which is important for using of the numerical data given in SDSS tables.

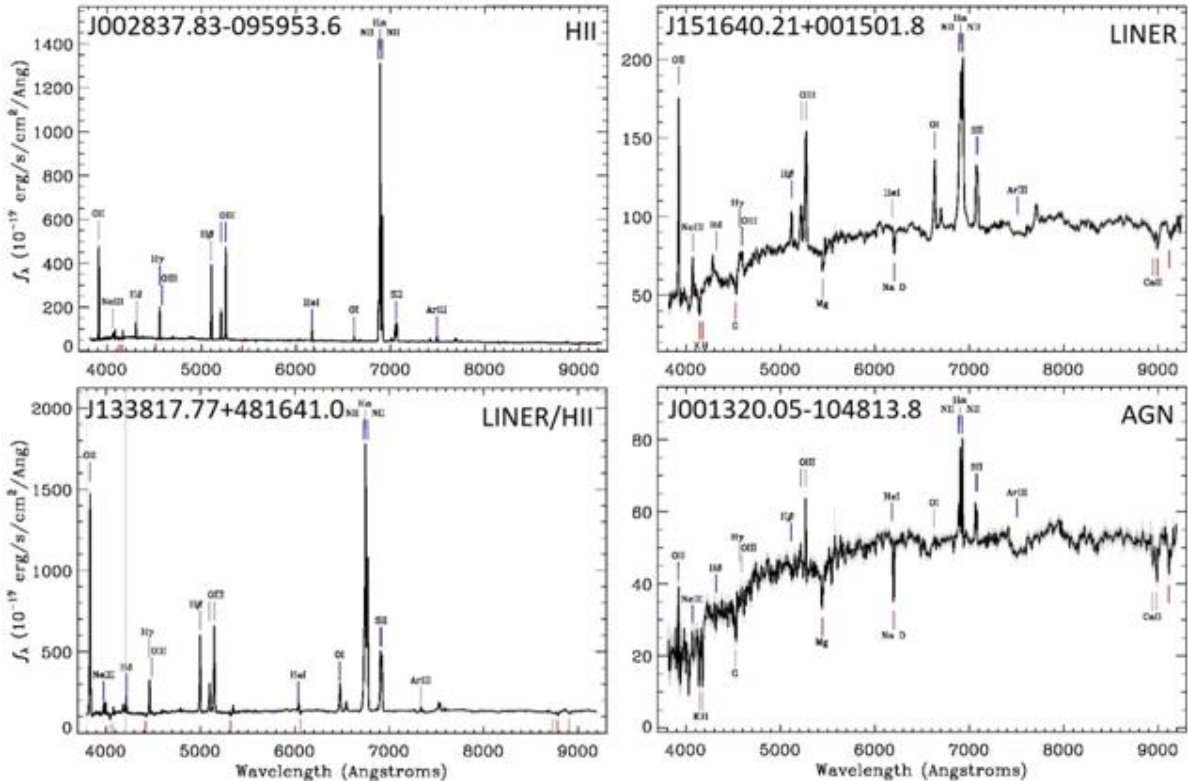


Figure 5. Examples of spectra used for reclassification of "LINERs".

After identifications of the lines we decided which of them should be used to build diagnostic diagrams. As a result we could build diagnostic diagram using

$[\text{OIII}]/H_{\beta}$ and $[\text{NII}]/H_{\alpha}$ ratios for 84 objects, diagnostic diagram using $[\text{OIII}]/H_{\beta}$ and $[\text{SII}]/H_{\alpha}$ ratios for 83 objects and $[\text{OIII}]/H_{\beta}$ and $[\text{OI}]/H_{\alpha}$ ratios for 81 objects (figure 4).

On diagnostic diagrams the narrow-line AGN separated into 3 main groups (HII, Sy, LINER). In addition, there are objects in intermediate areas, which have been classified as composites (S.Veilleux et al. 1987) having both AGN and HII features. As a result, 54% of LINERs changed their classification (table 3).

Table 3. Classification of LINERs using SDSS DR14.

Classification in VCV-13	Classification using SDSS DR14 spectra	Number of objects
LINER	Abs	6
LINER	AGN	3
LINER	Em	39
LINER	Sy1.5	1
LINER	Sy1.8	1
LINER	HII	88
LINER	HII/Sy1.9	4
LINER	HII/Sy2	1
LINER	LINER	20
LINER	LINER/HII	8
LINER	LINER/Sy1.9	5
Total		176

In table 4 we give data on our investigated sources: coordinates, redshifts, magnitudes and our classification. In table 3 we have objects with classifications Abs, Em or just AGN. These objects have poor quality spectra in SDSS DR14 and we do not change their final classification, because older spectra might be better than spectra from SDSS (though not always obvious). Therefore, we leave them as "LINERs" before any better quality spectrum may make re-classifying the type. This brings the number of LINERs to 81, just 46% of the original list.

Table 4. List of VCV-13 "LINERs" and their re-classification.

N	Veron coordinate		umag	gmag	rmag	imag	zmag	Redshift	Classification
			mag	mag	mag	mag	mag		
1	3.3338	-10.8036	17.533	15.835	15.035	14.591	14.24	0.05175	AGN
2	3.9925	-0.3033	17.047	15.098	14.252	13.902	13.61	0.03937	LINER
3	4.9121	-9.6739	17.981	15.854	14.801	14.296	13.919	0.08481	LINER
4	5.3321	0.6336	20.212	19.366	18.779	18.325	18.129	0.23378	HII

5	6.045	-1.0203	17.7	15.767	14.865	14.437	14.135	0.06489	LINER
6	7.1575	-9.9981	17.618	16.839	16.495	16.073	15.929	0.04965	HII
7	7.3196	15.1836	20.712	19.846	19.203	18.76	18.721	0.21605	HII
8	10.3237	15.8581	19.768	17.811	16.859	16.36	15.986	0.08015	LINER
9	10.7404	-1.0797	20.99	20.345	19.562	19.242	18.92	0.36317	HII
10	11.2629	-0.5347	21.112	19.847	19.173	18.869	18.725	0.19885	HII
11	13.5729	-0.7017	21.293	19.957	19.317	18.994	18.747	0.14516	HII
12	13.7129	0.6031	20.358	19.774	18.99	18.782	18.462	0.32008	HII
13	13.7875	-1.0461	17.003	15.083	14.208	13.812	13.508	0.04571	LINER
14	14.4617	-1.1503	20.694	20.385	19.811	19.657	19.52	0.41801	LINER
15	14.5033	0.4792	17.708	16.796	16.454	16.076	16.026	0.08012	HII
16	14.72	-0.775	19.746	19.179	18.709	18.587	18.28	0.26579	HII
17	15.3325	-0.7797	20.663	19.713	19.05	18.553	18.508	0.19905	HII
18	16.2033	-0.8947	18.546	17.234	16.664	16.281	16.107	0.06488	HII
19	17.9475	0.3389	19.858	19.06	18.482	18.223	17.875	0.25391	HII
20	21.2254	0.9931	21.418	20.253	19.501	19.011	18.823	0.23176	HII
21	24.7204	-10.4531	18.979	16.752	16.165	15.7	15.508	0.04823	LINER
22	25.7604	13.645	21.116	18.412	16.687	16.033	15.407	0.00286	LINER/HII
23	28.4325	0.1839	17.954	16.631	15.957	15.455	15.18	0.08209	HII
24	29.1421	-7.8078	19.375	17.152	16.091	15.625	15.26	0.1127	LINER
25	29.1829	-10.0128	20.895	20.062	19.441	18.997	18.896	0.15753	HII
26	30.0746	0.2417	19.679	18.796	18.356	17.954	17.955	0.0769	HII
27	30.6071	-1.0378	20.251	19.459	18.959	18.525	18.564	0.19136	HII
28	31.0246	-8.125	17.875	15.719	14.737	14.198	13.763	0.03325	LINER
29	31.0929	-9.6325	19.773	18.407	17.627	17.031	16.808	0.19189	HII
30	32.3371	-10.1331	15.667	13.549	12.512	12.044	11.699	0.01286	LINER
31	34.3475	-0.5217	20.904	19.879	19.166	18.813	18.589	0.18604	HII
32	36.2	-0.5267	20.678	19.765	19.458	19.287	19.147	0.02618	LINER
33	36.5283	-0.3317	15.246	13.757	12.853	12.461	12.137	0.02131	LINER
34	38.5583	-0.46	18.843	17.896	17.368	16.906	16.736	0.11149	HII
35	42.7396	0.3694	17.299	16.513	16.09	15.796	15.608	0.04421	HII
36	45.7383	-8.495	18.602	17.42	16.771	16.239	16.04	0.10555	HII
37	46.1267	-7.6689	19.434	18.55	18.006	17.578	17.427	0.1514	HII
38	48.8854	1.215	20.872	19.864	18.968	18.385	18.089	0.20347	HII
39	58.0837	-0.9731	17.255	15.359	14.391	13.899	13.507	0.03889	AGN
40	58.6679	-6.5942	20.351	19.851	19.242	18.933	18.628	0.25112	HII
41	61.9996	-6.3306	19.682	17.607	16.803	16.214	15.904	0.12069	HII
42	116.7583	41.5361	16.498	14.433	13.594	13.13	12.822	0.0286	LINER
43	120.915	44.2325	20.035	19.345	18.781	18.43	18.306	0.19353	HII
44	121.4404	7.5903	16.435	14.973	14.293	13.871	13.6	0.05327	Sy1.5
45	122.5971	42.2739	17.429	15.34	14.32	13.84	13.515	0.0635	LINER
46	125.8404	4.3725	15.461	13.717	12.698	12.434	12.022	0.03106	LINER
47	128.0258	49.0417	18.698	17.614	17.093	16.618	16.495	0.09113	HII
48	128.4762	51.6947	18.488	17.297	16.685	16.248	16.025	0.06549	HII
49	129.1879	53.0431	19.52	18.585	17.985	17.542	17.355	0.13818	HII

50	131.2358	42.9761	16.759	14.822	13.926	13.478	13.185	0.05402	LINER
51	131.815	51.2456	16.861	15.726	15.156	14.874	14.594	0.02754	HII
52	133.705	57.67	16.345	14.831	13.96	13.526	13.133	0.01423	HII
53	134.9446	1.1367	18.811	18.255	17.861	17.438	17.555	0.19848	HII
54	135.9671	-0.8978	18.341	16.934	16.147	15.712	15.399	0.088	HII
55	142.7779	49.08	16.407	14.92	14.246	13.879	13.578	0.03393	LINER/HII
56	143.4421	10.1525	15.137	12.98	12.037	11.542	11.183	0.01078	LINER
57	144.6621	41.3592	19.274	18.853	18.361	18.12	17.868	0.25702	Sy1.8
58	147.125	55.6394	17.891	16.808	16.325	15.96	15.744	0.04529	HII
59	149.995	3.0397	18.788	17.476	16.87	16.337	16.163	0.09059	HII/Sy2
60	151.17	0.3697	17.745	15.882	15.05	14.656	14.326	0.04459	LINER
61	151.5071	34.9031	17.799	16.108	15.088	14.625	14.267	0.09936	LINER/Sy1.9
62	154.7437	37.3003	17.444	16.264	15.703	15.318	15.123	0.04758	HII
63	157.4875	40.0569	19.47	17.776	16.991	16.537	16.309	0.09418	LINER
64	157.9525	58.3267	17.95	16.042	15.284	14.875	14.617	0.092	LINER
65	159.3654	2.0892	18.194	16.347	15.457	15.018	14.67	0.07292	LINER
66	161.2879	0.0758	19.347	17.297	16.321	15.828	15.545	0.09437	LINER
67	164.5983	-1.0906	19.944	19.769	19.128	17.999	17.853	0.18697	HII
68	167.4187	-1.0217	19.644	18.29	17.547	17.036	16.838	0.10885	HII
69	167.8046	28.6964	16.309	14.206	13.266	12.848	12.495	0.02875	LINER/Sy1.9
70	169.4721	-0.0075	18.335	17.366	16.997	16.591	16.538	0.09613	HII
71	170.5742	59.0744	13.644	12.171	11.518	11.195	10.988	0.00524	LINER/HII
72	173.6929	2.9208	16.569	15.561	15.004	14.712	14.48	0.02875	HII
73	175.5146	0.86	19.141	18.46	18.004	17.658	17.496	0.24509	LINER
74	176.5508	20.3914	15.359	13.431	12.589	12.16	11.894	0.02313	LINER/Sy1.9
75	176.5896	30.4936	17.581	16.2	15.884	15.689	15.583	0.04049	HII
76	177.1912	29.6414	16.8	15.013	14.075	13.528	12.997	0.0253	HII
77	179.4029	32.2781	15.149	13.597	12.678	12.222	11.907	0.01028	LINER
78	179.5046	-2.1772	18.14	16.224	15.282	14.855	14.482	0.08179	LINER
79	180.7646	60.5217	17.268	16.015	15.251	14.824	14.546	0.0653	LINER
80	182.3233	44.0903	16.403	14.825	14.306	14.027	13.841	0.03722	LINER
81	184.8496	44.0414	17.758	16.112	15.285	14.858	14.554	0.06744	LINER
82	186.3562	28.9439	16.987	15.727	15.111	14.734	14.521	0.0642	LINER
83	186.995	28.8289	17.741	16.115	15.342	14.932	14.672	0.05008	HII
84	187.8454	29.1364	15.136	13.691	12.901	12.472	12.102	0.01524	HII
85	188.9529	29.1942	16.992	15.367	14.571	14.121	13.804	0.06351	LINER
86	191.3971	28.7619	17.183	15.773	15.122	14.821	14.589	0.02318	LINER
87	193.0737	27.0856	17.126	15.386	14.591	14.205	13.922	0.02098	LINER
88	193.1933	0.2483	21.77	20.759	19.869	19.506	19.005	0.32878	HII
89	193.2212	29.2247	18.936	17.317	16.451	16.041	15.717	0.08475	LINER
90	196.5721	29.0631	15.724	13.971	13.136	12.737	12.472	0.02338	LINER
91	197.9092	29.2706	18.967	17.349	16.553	16.151	15.86	0.06073	HII
92	199.835	-2.4264	18.328	17.494	17.063	16.642	16.528	0.09745	HII
93	200.0608	33.1442	16.29	14.306	13.468	13.051	12.75	0.03606	LINER
94	202.8896	29.1203	19.108	17.617	16.836	16.417	16.129	0.07311	HII

95	203.0987	43.5933	19.225	17.624	16.744	16.25	15.905	0.12449	LINER/HII
96	203.2721	-1.0358	15.374	13.426	12.507	12.075	11.804	0.01235	LINER
97	203.3954	29.8225	17.881	16.441	15.696	15.252	14.879	0.03646	HII
98	204.3462	-0.5703	19.859	19.417	19.104	18.906	18.901	0.23609	HII
99	204.5742	48.2778	15.773	14.488	13.839	13.537	13.289	0.0277	LINER/HII
100	205.0133	29.1372	17.284	15.997	15.449	15.132	14.919	0.04469	LINER
101	205.0163	0.2853	19.818	18.969	18.4	17.969	17.764	0.23536	HII
102	205.4775	29.6828	18.319	16.47	15.551	15.045	14.649	0.04461	LINER
103	207.1329	28.825	17.436	15.69	14.817	14.359	14.043	0.06279	LINER
104	207.4558	29.1078	18.995	17.351	16.542	16.108	15.804	0.07726	LINER
105	208.075	31.4461	16.857	15.056	14.125	13.615	13.261	0.04519	LINER/Sy1.9
106	208.5358	29.0028	19.108	17.293	16.333	15.817	15.434	0.07942	LINER
107	209.3071	-0.5031	22.136	21.046	20.163	19.881	19.324	0.28028	HII
108	209.6463	28.8478	17.654	15.901	15.04	14.578	14.215	0.03847	LINER
109	209.6583	28.8658	17.398	15.728	14.9	14.476	14.142	0.03893	LINER
110	210.1362	28.6608	17.519	16.186	15.54	15.114	14.87	0.0691	HII/Sy1.9
111	211.0758	3.6211	20.464	19.456	18.895	18.505	18.449	0.23208	LINER/HII
112	211.1446	-0.1333	20.312	19.605	19.076	18.91	18.461	0.30378	HII/Sy1.9
113	212.4383	29.6442	19.26	17.585	16.645	16.158	15.794	0.06427	LINER
114	212.6725	13.5581	16.757	14.902	14.062	13.637	13.318	0.01622	LINER
115	216.2342	-0.3761	17.647	17.078	16.763	16.39	16.356	0.07895	HII
116	216.6617	1.3594	19.88	19.293	18.577	18.389	17.985	0.3288	HII
117	216.7942	29.0603	17.934	16.416	15.643	15.252	14.939	0.03901	HII
118	217.8021	2.1767	18.444	17.285	16.624	16.148	15.951	0.1105	LINER
119	218.1662	36.3025	15.445	13.564	12.485	11.975	11.545	0.01325	LINER
120	218.9542	42.5392	18.042	16.267	15.427	15.019	14.696	0.07075	HII
121	219.8971	59.2739	18.542	17.62	17.253	17.059	16.917	0.02905	HII
122	221.5992	4.6608	19.114	18.134	17.51	17.136	16.975	0.15717	HII
123	223.6987	1.0975	18.896	17.819	17.188	16.709	16.586	0.16351	HII
124	224.7533	29.5786	18.721	17.448	16.87	16.53	16.313	0.08078	HII
125	224.9037	29.2508	18.887	17.451	16.827	16.469	16.198	0.0622	HII
126	225.1987	28.7961	18.399	17.26	16.719	16.363	16.158	0.05728	HII
127	226.7229	12.8586	16.233	14.648	13.888	13.514	13.235	0.02157	LINER/HII
128	226.8329	29.5653	17.899	16.379	15.598	15.945	14.902	0.05822	LINER/HII
129	226.91	28.8139	19.234	17.671	16.94	16.535	16.231	0.05863	LINER
130	227.445	57	13.91	12.35	11.606	11.241	10.886	0.00254	LINER
131	227.6233	-2.1686	16.72	14.696	13.744	13.249	12.922	0.03717	LINER
132	228.8779	2.7508	17.741	16.699	16.205	15.88	15.666	0.03812	HII
133	229.1675	0.2506	17.229	15.679	14.801	14.332	14	0.05259	LINER
134	229.3871	0.4681	19.833	18.288	17.517	17.016	16.721	0.05219	HII
135	229.4792	57.1994	20.125	19.348	18.622	18.395	17.948	0.31451	HII
136	229.5258	42.7453	16.278	15.298	14.757	14.318	14.013	0.04027	HII
137	229.5892	-1.6536	18.725	16.808	15.732	15.188	14.75	0.054	LINER
138	230.08	29.1053	18.9	17.429	16.673	16.261	15.993	0.07885	LINER
139	230.7108	29.1772	18.57	17.006	16.2	15.765	15.46	0.07841	LINER

140	231.5254	41.6708	15.442	13.759	12.894	12.659	12.168	0.00829	LINER/Sy1.9
141	233.0404	58.9053	17.636	15.563	14.608	14.178	13.843	0.06807	LINER
142	236.4304	29.7397	18.774	17.223	16.484	16.089	15.784	0.0626	LINER
143	238.2108	53.6856	19.055	18.49	18.001	17.868	17.397	0.28671	HII/Sy1.9
144	238.4183	43.7344	17.56	15.998	15.229	14.797	14.5	0.0579	HII/Sy1.9
145	238.5792	12.1253	16.761	15.653	15.034	14.683	14.42	0.03497	HII
146	241.1242	29.3267	20.11	18.313	17.377	16.886	16.547	0.08171	LINER
147	242.3129	49.0803	18.598	17.526	16.891	16.435	16.28	0.1112	HII
148	242.4812	43.1292	17.257	15.491	14.664	14.16	13.761	0.03288	LINER
149	243.1833	52.3317	19.502	18.84	18.373	18.021	17.862	0.1817	HII
150	243.2446	29.5567	17.599	16.319	15.617	15.209	14.922	0.06102	HII
151	243.3571	52.5697	20.124	19.339	18.739	18.467	18.13	0.29835	HII
152	244.3837	-0.2836	18.793	17.523	16.928	16.5	16.263	0.0575	HII
153	245.2383	6.7464	19.708	18.181	17.345	16.76	16.464	0.0595	HII
154	246.855	42.6797	15.827	13.815	12.963	12.561	12.273	0.03138	LINER
155	249.085	-0.1411	18.874	17.892	17.44	17.066	16.941	0.08748	HII
156	251.2121	41.9294	19.248	18.197	17.64	17.201	17.067	0.09678	HII
157	251.6708	29.835	18.663	16.988	16.185	15.715	15.388	0.06221	HII
158	252.7612	42.2206	19.39	18.785	18.308	18.05	17.752	0.25374	HII
159	253.4671	62.1969	17.834	16.736	16.177	15.629	15.509	0.10603	HII
160	257.3275	62.2919	19.831	19.059	18.563	18.237	18.127	0.19111	HII
161	258.075	64.9853	19.591	18.975	18.604	18.333	18.285	0.18371	HII
162	313.9021	-0.6364	17.426	15.433	14.586	14.17	13.83	0.05353	AGN
163	315.5829	-6.1858	19.349	18.857	18.614	18.049	18.163	0.09702	HII
164	320.2725	-0.3192	20.606	19.911	19.546	19.335	19.266	0.21421	HII
165	323.0746	-0.6425	19.852	19.128	18.714	18.628	18.465	0.05111	LINER
166	323.885	-7.7956	21.654	20.564	19.752	19.426	18.816	0.31088	HII
167	328.2708	-7.1853	16.907	14.938	14.019	13.572	13.247	0.05895	LINER
168	328.4796	-0.4067	20.498	19.635	18.858	18.363	18.109	0.23262	HII
169	330.0575	-6.98	16.748	15.032	14.355	14.007	13.732	0.05692	LINER
170	332.8646	-0.0506	17.866	15.752	14.743	14.279	13.916	0.05235	LINER
171	342.6925	-1.0672	20.669	20.363	19.499	19.129	18.7	0.37498	HII
172	348.7567	0.0725	17.22	15.645	14.862	14.463	14.211	0.05122	LINER
173	349.535	-0.3906	16.028	14.106	13.212	12.796	12.443	0.02927	LINER
174	350.2242	1.0997	21.557	20.025	19.088	18.587	18.207	0.2605	HII
175	357.3742	-0.2667	19.984	19.044	18.389	17.942	17.738	0.2199	HII
176	359.1717	-1.0822	20.345	19.775	19.072	18.731	18.309	0.29149	HII

References

- Abazajian, K., Adelman-McCarthy, J. K., Agüeros, M. A., et al. 2003, AJ, 126, 2081
 Abazajian, K., Adelman-McCarthy, J. K., Agüeros, M. A., et al. 2004, AJ, 128, 502
 Abazajian, K., Adelman-McCarthy, J. K., Agüeros, M. A., et al. 2005, AJ, 129, 1755
 Abazajian, K., Adelman-McCarthy, J. K., Agüeros, M. A., et al. 2009, ApJS, 182, 543

- Adelman-McCarthy, J. K., Agüeros, M. A., Allam S. S., et al. 2006, ApJS, 162,38
Adelman-McCarthy, J. K., Agüeros, M. A., Allam S. S., et al. 2007, ApJS, 172,634
Adelman-McCarthy, J. K., Agüeros, M. A., Allam S. S., et al. 2008, ApJS, 175,297
Croom, S. M., Smith, R. J., Boyle, B. J., et al. 2001, MNRAS, 322, L29
Croom, S. M., Smith R. J., Boyle B. J., et al. 2004, MNRAS, 349, 1397
De Veny, J. B., Osborn W. H., Janes K. 1971, PASP, 83, 611
Fan, X., Strauss, M. A., Schneider, D. P., et al. 1999, AJ, 118, 1
Ho, L. C., Filippenko, A. V., Sargent, W. L. W., 1997, Proceedings of IAU Colloquium No. 159
Véron-Cetty, M.-P., Véron, P., 2010, A&A, 518, A10
Veilleux, S., Osterbrock, D.E. 1987, ApJS 63, 295
Mickaelian, A. M., Harutyunyan, G. S., Sarkissian, A., 2018, Astronomy Letters, 44, 6
Reines, A. E., Greene, J. E., Geha M., 2013, AJ, 755, 2